Breast cancers that disseminate to bone marrow acquire aggressive phenotypes through CX43-related tumor-stroma tunnels

Saptarshi Sinha,[1] Brennan W. Callow,[2] Alex P. Farfel,[2] Suchismita Roy,[1] Siyi Chen,[2] Maria Masotti,[3] Shrila Rajendran,[2] Johanna M. Buschhaus,[2,4] Celia R. Espinoza,[1] Kathryn E. Luker,[2,5] Pradipta Ghosh,[1,6,7,8] and Gary D. Luker[2,4,5]

[1]Department of Cellular and Molecular Medicine, School of Medicine, UCSD, La Jolla, California, USA. [2]Center for Molecular Imaging, Department of Radiology, [3]Biostatistics, School of Public Health, [4]Department of Biomedical Engineering, and [5]Biointerfaces Institute, University of Michigan, Ann Arbor, Michigan, USA. [6]Moores Comprehensive Cancer Center, [7]Department of Medicine, [8]School of Medicine, and Veterans Affairs Medical Center, UCSD, La Jolla, California, USA.

Estrogen receptor-positive (ER+) breast cancer commonly disseminates to bone marrow, where interactions with mesenchymal stromal cells (MSCs) shape disease trajectory. We modeled these interactions with tumor-MSC co-cultures and used an integrated transcriptome-proteome-network-analyses workflow to identify a comprehensive catalog of contact-induced changes. Conditioned media from MSCs failed to recapitulate genes and proteins, some borrowed and others tumor-intrinsic, induced in cancer cells by direct contact. Protein-protein interaction networks revealed the rich connectome between "borrowed" and "intrinsic" components. Bioinformatics prioritized one of the borrowed components, *CCDC88A*/GIV, a multi-modular metastasis-related protein that has recently been implicated in driving a hallmark of cancer, growth signaling autonomy. MSCs transferred GIV protein to ER+ breast cancer cells (that lack GIV) through tunnelling nanotubes via connexin (Cx)43-facilitated intercellular transport. Reinstating GIV alone in GIV-negative breast cancer cells reproduced approximately 20% of both the borrowed and the intrinsic gene induction patterns from contact co-cultures; conferred resistance to anti-estrogen drugs; and enhanced tumor dissemination. Findings provide a multiomic insight into MSC→tumor cell intercellular transport and validate how transport of one such candidate, GIV, from the haves (MSCs) to have-nots (ER+ breast cancer) orchestrates aggressive disease states.

Introduction

Estrogen receptor-positive (ER+) breast cancer, the most common subtype, preferentially disseminates to bone and bone marrow (1, 2). Bone metastases remain incurable and cause debilitating symptoms, e.g., pain, fractures, and life-threatening hypercalcemia (3). Bone marrow harbors disseminated tumor cells (DTCs) in breast cancer. DTCs may persist in a clinically occult state for decades before proliferating and potentially traveling to other organs to produce delayed recurrences in approximately 40% of patients with ER+ breast cancer (4). Recurrent disease is more aggressive, relatively resistant to treatment, and currently incurable. Little progress has been made in treating breast cancer that has already disseminated to bone (5), largely because we lack a comprehensive understanding of molecular mechanisms that make ER+ breast cancer cells more aggressive in the bone marrow niche (6).

Interactions with stromal cells in the bone marrow environment are proposed to shape key functions of breast cancer cells that determine disease progression and outcomes (7). Mesenchymal stem cells (MSCs), a multipotent cell type that contributes to formation of bone, fat, and cartilage, are a major stromal cell type driving aggressive phenotypes of disseminated ER+ breast cancer cells in bone marrow. MSCs regulate ER+ breast cancer cells through mechanisms such as secreted cytokines and direct intercellular interactions (8). Work by us and others has established that direct interactions with MSCs, rather than soluble molecules, drive changes in gene expression and metabolism that promote cancer stem-like cell states, resistance to anti-estrogen drugs, and metastasis in ER+ breast cancer (9–11). Breast cancer cells and MSCs can establish channels of intercellular communication that transport molecules and organelles. Two major structures for intercellular communication include gap junctions and tunneling nanotubes (TNTs), both of which share connexin 43 (Cx43) as an essential molecular player. Gap junctions are intercellular channels comprised of various subsets of connexin proteins (12). Lymph node and systemic metastases in breast cancer and other malignancies upregulate gap junctions and Cx43, suggesting these structures contribute to essential steps in the metastatic cascade (13). TNTs are actin-rich long, thin tubes that may form between cells of the same or different types, thereby allowing long-range communication via the exchange of materials (14, 15). TNTs serve as "exchange freeways" for a broad range of intracellular contents, including microRNAs, proteins, and organelles. Such exchanges,

Conflict of interest: GDL has received research materials from Spexis. All other authors declare no competing interests.

Submitted: March 29, 2023; **Accepted:** October 24, 2024; **Published:** October 31, 2024.
Reference information: *J Clin Invest*. 2024;134(24):e170953.
https://doi.org/10.1172/JCI170953.

between tumor cells or between tumor and stromal or immune cells (8, 16, 17) shape drug resistance of cancer cells; regulate proliferation; and promote metastasis.

Despite these insights, only a limited number of molecules transferred from MSCs via gap junctions or TNTs have been implicated in aggressive phenotypes of breast cancer cells, whereas the identity of most remains unknown. We tackle this knowledge gap by performing a comprehensive multiomic network analysis to identify molecules and biologic processes regulated by direct contact between bone marrow MSCs and ER+ breast cancer cells. We identified genes and proteins that cancer cells acquire from MSCs through direct transfer ("borrowed" components) and additional molecules induced because of such transfer ("intrinsic" components). We used bioinformatic approaches to explore the implications of these gene expression changes on patient outcome and subsequently prioritized one borrowed gene/protein (*CCDC88A*/GIV) to explore further and validate through a series of in vitro and in vivo studies. Our findings establish a comprehensive resource for changes induced in ER+ breast cancer cells by contact with bone marrow MSCs and pinpoint GIV as a promising target to overcome aggressive phenotypes acquired by breast cancer cells in bone marrow.

Results

Multiomic analysis of close contact between ER+ breast cancer cells and MSCs. DTCs in bone marrow displace hematopoietic stem cells from supportive niches (18), where they establish direct contact with various subsets of MSCs and eventually gain aggressiveness. To identify how MSCs may impact ER+ breast cancer cells through direct contact, we used a 2D co-culture model combining MCF7 or T47D human ER+ breast cancer cells with human HS5 or HS27a MSCs in a 1:9 ratio (Figure 1A). After 3 days of co-culture in medium with low serum and physiologic concentrations of glucose, we recovered cancer cells using EpCAM immunomagnetic beads, capitalizing on expression of EpCAM exclusively on tumor cells of epithelial origin. We previously showed that such EpCAM-based immunoisolation has negligible MSC contamination (19) and confirmed through rigorous characterization studies showing that tumor cells subjected to such contact culture gain advantageous features such as metabolic plasticity (20), resistance to estrogen-targeted therapies, and enhanced survival of disseminated tumor cells early in the metastatic process (19, 21). To control for effects of soluble molecules produced by MSCs, we cultured MCF7 or T47D cells for 3 days in conditioned medium from MSCs (Figure 1A). We used monocultures of MSCs and tumor cells as additional comparator groups. We analyzed all samples by bulk RNA sequencing; we also analyzed mono- and contact cultured MCF7 cells by TMT proteomics.

MCF7 cells exposed to contact culture, but not conditioned media, correlated with substantial lowering of a previously defined 49-gene signature for tumor cell dormancy (Figure 1B); low dormancy scores confer an approximately 2.1-fold increase in risk of recurrence in 4 independent cohorts of patients with ER+ breast cancers ($P < 0.000005$) (22). These findings suggest that our co-culture model captures key transcriptomic changes in ER+ breast cancer cells of translational relevance to more aggressive disease in patients.

We carried out combinatorial multiomics analyses to determine what proteins or transcripts expressed highly in MSCs are borrowed by MCF7 cells. To this end, we first created a catalog of genes differentially expressed (DEGs; upregulated) in MSCs, but not in MCF7 cells (MCF7 vs. HS5; $n = 1471$; Figure 1C). This catalog served as a denominator for all likely candidate genes that a tumor cell may lack originally but acquire from MSCs via intercellular communication. Next, we performed pairwise DEG analysis on the other MCF7 samples subjected to different co-culture conditions. Direct contact co-culture induced many genes ($n = 482$) and proteins ($n = 295$) (Figure 1C). Conditioned media induced few genes in cancer cells ($n = 13$; Figure 1C). An overlay showed the following: (a) Exposure to conditioned media alone induced only a single unique protein/transcript in MCF7 cells, implying soluble mediators or exosomes as potential modes of communication; (b) By contrast, contact culture accounted for 487 unique proteins/transcripts, implying direct contact as the major mode of tumor-MSC communication and the largest share of uniquely induced genes; (c) Contact culture increased 242 unique proteins/transcripts (39 transcripts and 203 proteins with no proteome-transcriptome overlap) in MCF7 cells. These transcripts/proteins were not highly expressed in HS5 cells. We presumed this last category to be tumor cell–intrinsic response to contact culture, unlikely to be transferred directly from MSCs to breast cancer cells. We note that neither the experimental design nor the analytical steps can conclude definitively whether transport of a given target occurred as a protein or as mRNA because unknown factors (transcript/protein half-life) likely confound such conclusions. Similarly, while we infer that 487 unique RNAs/proteins could be transferred during contact culture, i.e., borrowed directly by cancer cells from the MSCs, we cannot exclude some cancer cell–intrinsic contributions to the overall levels. We did observe, however, enrichment of the borrowed RNA/proteins for biological processes that govern tube morphogenesis, organization of extracellular encapsulated structures, and movement of anatomic structures in the context of multicellular systems (Figure 1D). Enrichment of these processes further suggests the potential for direct transfer of RNA/protein from MSCs to cancer cells through structures such as TNTs. Reactome and gene ontology analyses of the genes induced by conditioned media, contact culture and intrinsic response present a comprehensive picture of distinct modes by which MSCs shape behavior and function of cancer cells (Supplemental Figure 1; supplemental material available online with this article; https://doi.org/10.1172/JCI170953DS1). A similar analysis for transcripts and proteins downregulated during contact culture and when exposed to conditioned media revealed genes/proteins that reduce the dependence on ER signaling (Supplemental Figure 2). We provide a full catalog of all upregulated (Supplemental Data Set 1) and downregulated (Supplemental Data Set 2) genes/proteins during contact culture.

A gene signature of contact culture is prognostic and predictive in ER+ breast cancers. We noted 39 unique, upregulated genes identified by both RNA seq and TMT proteomics in MCF7 cells during contact co-cultures (Figure 1C). Direct contact culture uniquely upregulated almost all genes ($n = 38$; Figure 1C) except for one (*KYNU*) upregulated in conditioned media. Hierarchical clustering, an unsupervised learning technique used to group similar

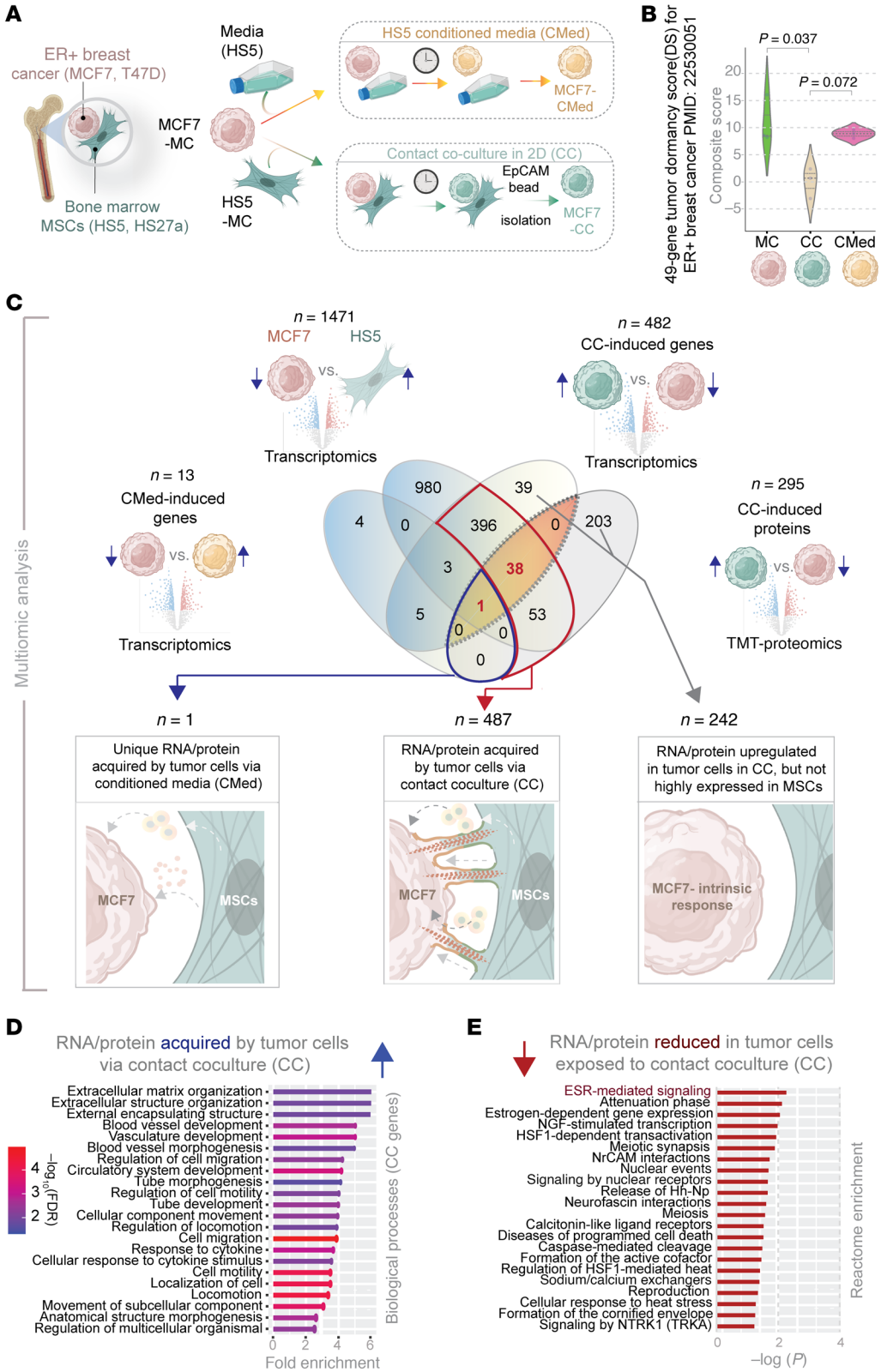

Figure 1. Multiomic analysis reveals RNA/protein acquired by ER+ breast cancer cells from MSCs in contact co-culture. (**A**) Experimental set up for recapitulating disseminated ER+ breast cancer cells in bone marrow amidst mesenchymal stem cells (MSCs). Two different types of co-culture models were used, one with conditioned media (CMed; top) and one with direct contact co-culture (CC; bottom). MC, monoculture. (**B**) Violin plots display the composite score of a 49-gene tumor dormancy score (DS) specific for ER+ breast cancers and previously validated in 4 independent cohorts to predict recurrence. (**C**) Top: Venn diagram depicts multiple DEG analyses between different indicated groups that catalog suppressed genes or proteins in contact co-culture (CC) or conditioned media (CMed) and overall differential gene expression between MCF7 versus HS5 bone marrow MSCs; bottom. Bottom: Genes/proteins induced in MCF7 cells in co-culture with HS5 MSCs are binned into 3 categories (connected by arrows) based on likely mechanisms for induction. Red = 39 uniquely upregulated transcripts in cancer cells in contact co-culture also identified by proteomics. (**D**) Gene ontology analysis (GO Biological processes) on transcripts and/or proteins acquired by MCF7 cells from MSCs during contact co-culture. See Supplemental Figure 1 for Reactome pathway and GO enrichment analyses on genes and/or proteins within each category in **C**. (**E**) Reactome analysis on transcripts and/or proteins reduced in MCF7 cells during contact co-culture with MSCs. See Supplemental Figure 2 for analyses on genes and proteins suppressed in cancer cells.

objects into clusters, showed the 39 genes grouped the samples into 2 distinct groups within a dendrogram: MCF7 cells subjected to culture in direct contact with HS5 cells (Figure 2A) clustered with the HS5 monoculture samples. By contrast, MCF7 cells cultured in conditioned media clustered with the MCF7 monoculture samples (compare MC and CMed; Figure 2A). A composite score of the levels of these 39 genes confirmed their statistically significant increase in contact cultures but not conditioned media (Fig-

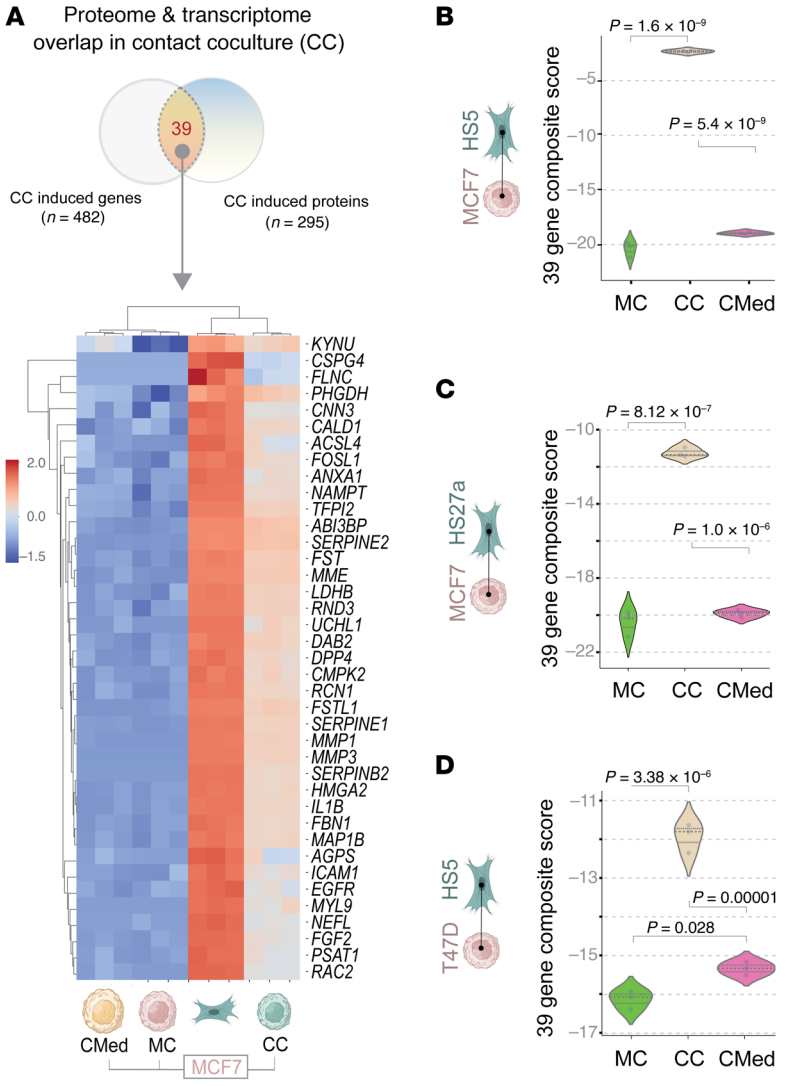

Figure 2. Genes uniquely upregulated in MCF7 tumor cells in contact co-culture with HS5 MSCs are identified reproducibly in other tumor-MSC co-culture models. (**A**) Heatmap displays hierarchical unsupervised clustering of samples used in Figure 1A using the 39 uniquely upregulated genes in cancer cells in contact culture. MC, monoculture. (**B**–**D**) Violin plots display the composite score of the 39 genes in **A** in various tumor cell-MSC co-culture models, e.g., MCF7↔HS5 (**B**), MCF7↔HS27a (**C**) and T47D↔HS5 (**D**). Statistical significance for **B**–**D** was assessed by 1-way ANOVA and the *P* values are corrected for multiple comparisons using Tukey's method.

ure 2B). This pattern of gene induction repeated when we swapped HS5 cells with another MSC line, HS27a, in co-cultures (Figure 2C) or swapped MCF7 cells with another ER+ breast cancer line, T47D (Figure 2D). These findings demonstrate that the 39-gene signature represents a conserved feature of how MSCs impact the properties or behavior of ER+ breast cancer.

The 39 genes showed enrichment of processes related to growth factor, PI3K/Akt, and *IL4/IL13* and *IL10*-centric tolerogenic cytokine signaling (Figure 3A), suggesting that acquisition of these 39 genes from MSCs may impact these aspects of cancer cell biology and/or behavior, including evasion of the immune system.

To test translational relevance of the 39-gene signature, we applied it to a publicly available dataset that prospectively tracked outcomes of ER+, Her2-negative breast cancers following neoadjuvant taxane-anthracycline chemotherapy (23) (Figure 3, B–E). Kaplan-Meier curves revealed that high levels of the contact culture signature correlated with significantly worse distant relapse-free survival in patients with ER+ (Figure 3B), but not ER–, breast cancers (Figure 3C). High levels of the close contact signature also predicted worse outcomes in patients with treatment resistant, but not treatment sensitive, disease (Figure 3, D and E). We reproduced these findings in an independent Her2-negative ER+ cohort from a large dataset, i.e., METABRIC (Molecular Taxonomy of Breast Cancer International Consortium; ref. 24), a landmark genomic and transcriptomic study of 2000 individual breast tumors (Figure 3, F and G). These findings establish that the 39 genes presumed to be borrowed by ER+ breast cancer cells via direct contact with MSCs carry translationally relevant information; they identify patients at greater risk for death from recurrent breast cancer.

Borrowed genes integrate with a cancer cell–intrinsic response during contact culture. Although TMT based proteomics can reliably detect as small as approximately one-tenth of the changes compared with label-free proteomics (25), it suffers from interference and distortion, which disproportionately impact low abundance proteins that often are the ones borrowed (26, 27). To circumvent this limitation and improve detection of relevant hits, we utilized a protein-protein interaction (PPI) network approach to identify relevant proteins, based on the assumption that the proteins function through meaningful interactions with each other. Briefly, we used the 39 proteins as seeds to build a PPI network consisting of 2743 proteins (Figure 4A). We overlaid the network-derived list with borrowed (n = 487) and intrinsic (n = 242) gene or protein sets (see Figure 1C) acquired by tumor cells via contact culture (n = 487) and genes or protein sets upregulated in tumor cells in contact culture but not highly expressed in MSCs. Generating the proteome network using the STRING database (see Methods) and then intersecting the proteome with the differential transcriptome increased signals (i.e., hits) by leveraging the sensitivity of transcriptomics and specificity of proteomics. This process produced a more focused network using 159 genes that ER+ breast cancer cells borrow from MSCs and 76 genes in the cancer cell intrinsic response group. Figure 4C displays the multilayer network connecting borrowed (pink) and intrinsic response (green) genes. Within the PPI network, 1482 nodes/proteins interacted within the borrowed layer and 835 nodes/proteins interacted within the intrinsic layer. The borrowed response interactome included Akt, growth factors and/or their receptors (*EGFR*, *VEGFA*, *WNT5A*), and integrins (Figure 4C), as noted earlier (Figure 3A). The borrowed network also revealed meaningful enrichment of other candidates, including the gap junction protein, *GJA1*/CX43, which has been impli-

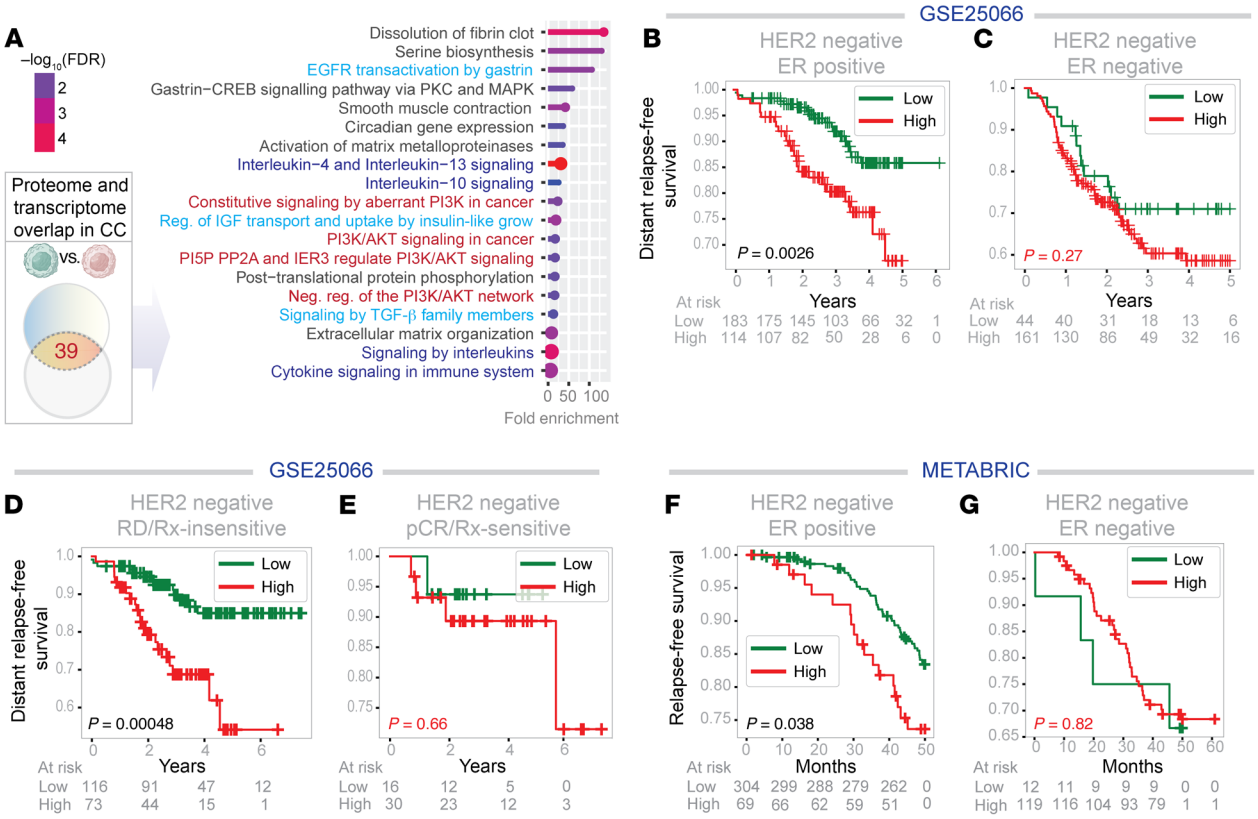

Figure 3. A contact culture signature derived from proteome-transcriptome overlap carries prognostic and predictive value in ER+ breast cancer. (**A**) Reactome pathways enriched in the 39 genes identified in Figure 1C. The PI3K/Akt signaling pathway (red), growth factor signaling pathways (teal blue), and the tolerogenic cytokine pathways (navy blue) are highlighted. (**B**–**G**) Kaplan-Meier survival plots on HER2-negative breast cancer patients from 2 independent cohorts with known outcomes over time (relapse/metastasis-free survival), stratified as high versus low expression of the 39-gene signature (see Methods). Statistical significance was assessed by log-rank analyses. RD, residual disease; PCR, pathologic complete response; Rx, treatment.

cated in establishing TNTs that facilitate exchange of molecules (28). The 2 layers shared 567 common nodes/proteins, indicating meaningful connectivity between 2 layers (*P* value of 0.00096 by hypergeometric test). The shared nodes were enriched for 3 prominent themes: membrane trafficking, immune signaling, and growth factor signaling (Figure 4D).

Findings suggest functional integration between the 2 components; the induction of one (the intrinsic cancer genes) may either enable functions of and/or reflect consequences of the other (the borrowed genes). Supplemental Data set 3 presents the edge and node list of the entire PPI network and various subnetworks.

CCDC88A/GIV as a key gene borrowed by cancer cells. To validate and/or characterize key components of the borrowed transcriptome/proteome and yet reduce the risk of noise (of STRING database) and artifacts (of 2D culture), we further refined this list (n = 159) generated using 2D cultures by leveraging a published dataset using the same cell lines as us except in 3D cultures (GSE152312) (Figure 5A) (29). We carried out this refinement with a 2-fold intention: (a) to enhance the physiological context and translational relevance because TNTs can form in 3D culture systems (30); and (b) to provide continuity between 2D and 3D TNT biology, which has been difficult to achieve in a field still in its infancy (31). Refinement gave a handful of genes (n = 19) also induced during 3D close contact culture in both MCF7 and T47D cells (Figure 5B). We noted that 2 of the 19 genes (*CCDC88A* and *EGFR*) are key components of a recently described phenomena, growth signaling autonomy, which endows breast tumor cells with plasticity and stemness (among other features) especially during hematogenous dissemination in metastasis (32, 33). Gene ontology (GO) analysis of these 19 genes revealed that *CCDC88A* (which encodes the protein Gα-interacting, vesicle-associated [GIV or Girdin]) is commonly shared among key processes upregulated in ER+ breast cells during reprogramming of signaling to adopt a mesenchymal state (34–38) (Figure 5C). Compared with MCF7 monocultures, 2D direct contact cultures, but not conditioned medium, markedly upregulated *CCDC88A* (Figure 5D). Focused analysis of the *CCDC88A/GIV*-subnetwork from the multilayer interactome (Figure 4C) revealed that the interactome of GIV could support numerous pathways and processes involved in cell projections and membrane domains (Figure 5E), suggesting that *CCDC88A* associates with direct intercellular contacts.

TNTs constitute a major pathway to transfer materials, including RNA and proteins, between cells of the same and different types (39) through direct intercellular contacts. Using interferometry microscopy, we identified numerous TNTs connecting MCF7 and HS5 cells (Figure 5F and Supplemental Figure 3). Images revealed significantly more heterotypic TNTs connecting MCF7 cells with HS5 or HS27a stromal cells than homotypic TNTs con-

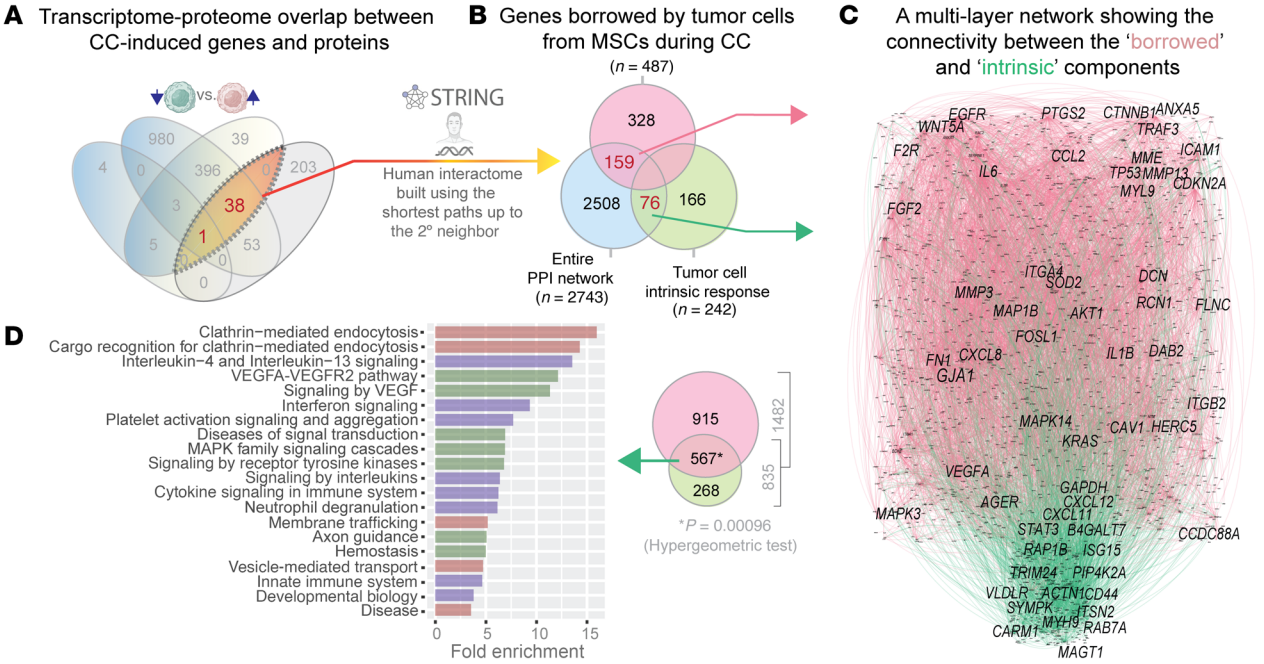

Figure 4. A multilayer network analysis to explore connectivity between the borrowed and intrinsic components of upregulated proteins in cancer cells after co-culture with MSCs. (**A**) Workflow for protein-protein interaction (PPI) network analysis using the 39 gene signature from Figure 1E as seeds for the STRING database. (**B**) Overlaps between the PPI network and genes/proteins from Figure 1C as likely borrowed from MSCs or upregulated in the cancer cell–intrinsic response during contact co-cultures. (**C**) Multilayer PPI network shows connectivity between borrowed (n = 159) and intrinsic (n = 76) proteins, with key nodes labeled. (**D**) Reactome pathways (left) enriched in 567 proteins shared between borrowed and intrinsic layers of the PPI network in **C**. Venn diagram (right) shows the total nodes in each layer and overlap.

necting MCF7 cells in monocultures (Figure 5F). TNT formation in contact cultures also associated with elevated expression of 2 proteins previously implicated as central factors essential for their formation: (a) the gap junction protein *GJA1* (28) (connexin 43, CX43; Figure 5G) and the TNT marker, *TNFAIP2* (40) (M-Sec; Figure 5H). To investigate whether gap-junction or TNT-facilitated intercellular communication is functional, we conducted the well-established calcein-AM transfer assay (41, 42). Co-culture of MCF7 cells stably expressing mCherry (recipients) with calcein-labeled HS5 MSCs (donors) or calcein-labeled MCF7 cells showed successful transfer of calcein into mCherry-labeled MCF7 cells (Supplemental Figure 4A). Both donor cells (HS5 and MCF7 cells) transferred calcein to recipient MCF7 cells. Although MCF7 cells formed both heterotypic and homotypic TNTs, transfer is markedly higher from MSCs (Supplemental Figure 4A). We also detected transfer from MCF7 cells to HSCs, albeit at lower efficiency (Supplemental Figure 4B). These results confirm that our 2D contact cultures allowed intercellular transport.

Together these findings suggest that TNTs in contact cultures could provide a route for breast cancer cells to borrow from MSCs certain RNAs and proteins, among which *CCDC88A*/GIV may be a central player in functional outcomes.

Transport of GIV/CCDC88A from MSCs to ER+ breast cancer cells. Although prioritized through computational rationale (Figure 5, A–E), we selected GIV (Figure 5B) because of 3 key reasons: First, as a large multi-modular protein that integrates signals from diverse classes of receptors and signaling pathways, GIV drives tumor cell aggressiveness — stemness (43), survival after DNA damage (44), invasiveness (44), chemoresistance (45), and acquisition of metastatic potential (46) — in multiple cancers, including breast (47), and is considered to be a metastasis-related protein (48) (Figure 6A). Second, unlike stromal cells (49, 50) and triple-negative breast cancers, which express high levels of GIV, ER+ breast cancer cells, such as MCF7 and T47D, lack GIV (51) due to an alternative splicing event (intron 19 retention) that leads to the loss of the resultant transcript to nonsense-mediated decay. The concept of haves (MSCs) lending GIV to have-nots (ER+ tumor cells) for potential gain in metastatic potential by the latter appeared interesting. Consistent with this concept, prior studies demonstrated that patients with ER+ breast cancers do express GIV, and such expression correlates with more metastasis and poorer survival (52, 53). Third, GIV has recently been shown to be a key orchestrator of secretion-coupled autonomy (32), wherein cancer cells may secrete and sense their own growth factors to survive. Proteomic studies confirmed that GIV enabled autocrine growth factor signaling autonomy specifically within the EGF/EGFR system (32). We note that EGFR is one of the initially identified list of 39 borrowed RNAs and proteins in contact culture (Figure 2A). EGFR remained on the list even after the 3D contact culture refinement (Figure 5A) as one of the 19 borrowed genes, alongside *CCDC88A* (Figure 5B).

GIV protein was virtually undetectable in lysates from monocultures of 3 different ER+ breast cancer cells but detected as a full-length protein (~250 kDa) in cells recovered with EpCAM-based immunocapture and lysis following 3 days in contact cultures with HS5 cells (Figure 6B). GIV protein was detected by

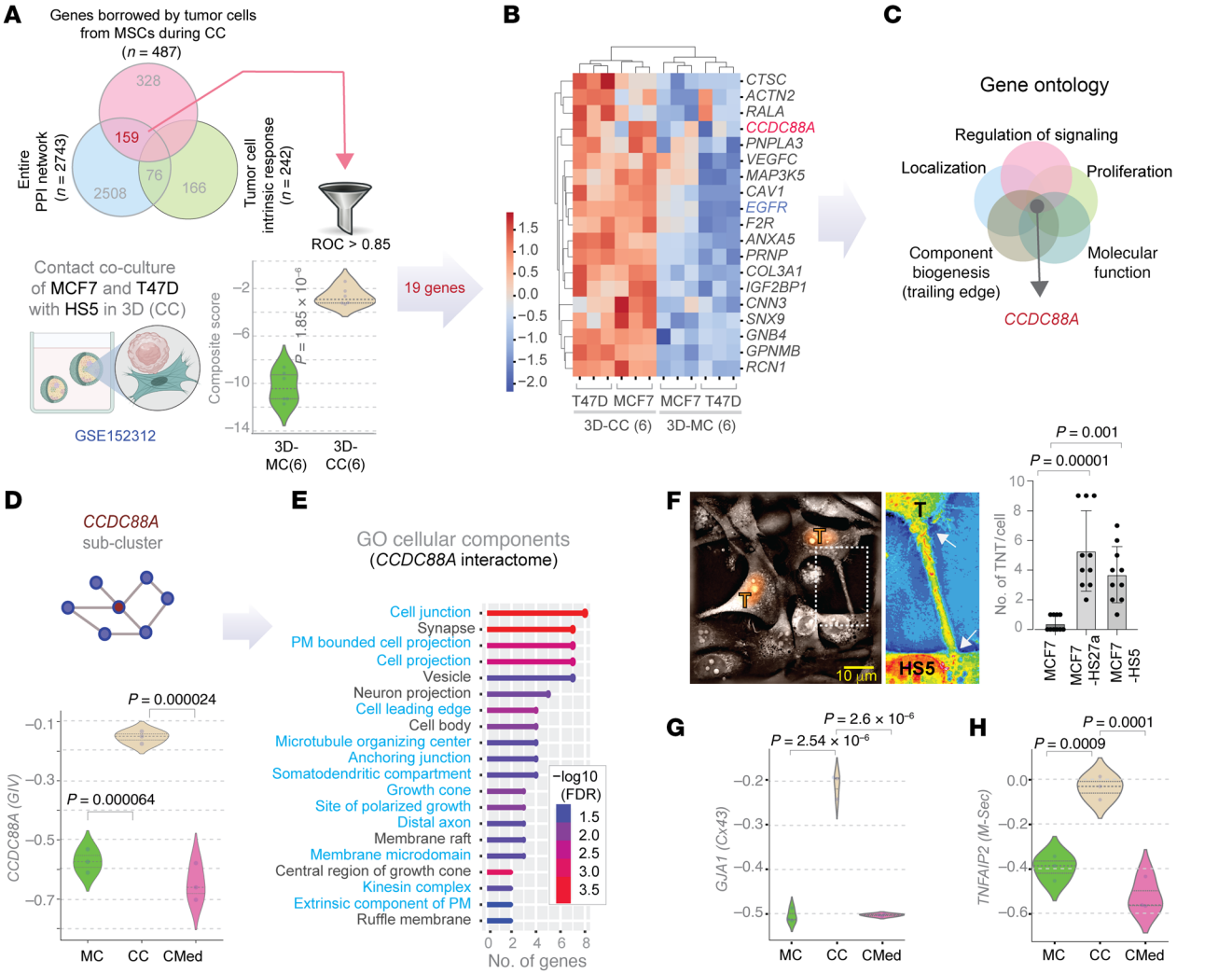

Figure 5. Integration of 2D and 3D co-culture–derived omics pinpoints GIV as a central orchestrator of the co-culture borrowed gene signature. (**A**) The 158 borrowed genes from our 2D co-cultures were further filtered using a public dataset from 3D co-cultures of MCF7 and T47D cells with HS5 MSCs. Threshold ROC AUC > 0.85 identified 19 genes. Violin plot shows the composite score for these 19 genes in 3D monoculture (MC) versus contact (CC) cultures. (**B**) Heatmap of *z* score–normalized expression of the 19 genes. (**C**) Gene ontology (GO) analyses identify *CCDC88A* as an invariant player across processes enriched within the 19 genes. (**D**) Shows induction of *CCDC88A* in MCF7 cells in contact coculture (CC) but not conditioned media (CMed). Only significant *P* values are displayed (Welch's *t* test). (**E**) Graph displays GO cellular components enriched in the *CCDC88A*/GIV-subcluster in **C**. Blue highlights denote processes required for transport via tunneling nanotubes. (**F**) MCF7 cells (red nuclei; "T") connected with a nanotube to HS5 MSCs in contact coculture (left). Boxed area is magnified on the right. Arrows mark the nanotube. Supplemental Figure 3 shows additional images. Bar plots (right) show average number of TNTs in each condition per field. (**G** and **H**) Violin plots show induction of *GJA1* (**G**) and *TNFAIP2* (**H**) in MCF7 cells in contact co-culture (CC) but not in conditioned media (CMed). *P* values for **A**, **F**, **G**, and **H** were derived by 1-way ANOVA and corrected for multiple comparisons by Tukey's method.

immunoblotting in MCF7 cells lysed immediately after separation from HS5 cells, but not after 24 to 96 hours of additional culture after separation (Figure 6C). These findings indicate that once acquired, cancer cells rapidly lose GIV after return to monoculture. ER+ breast cancer cells require ongoing close contact with MSCs to maintain levels of GIV.

To confirm whether MCF7 cells acquire GIV from HS5 cells and determine whether transport occurred as transcripts or proteins, we stably expressed short hairpin RNA (shRNA) targeting GIV in either MCF7 or HS5 cells and put them in contact culture with each other in various combinations (see Figure 6D). Batch populations of cells showed approximately 80% depletion of GIV in HS5 cells (Figure 6E). Contact cultures of control MCF7 and HS5 cells showed expected upregulation of full-length GIV in MCF7 cells (Figure 6; lane 3). Contact cultures of MCF7-shGIV and HS5 cells still showed increased amounts of GIV protein, indicating that shRNA against *CCDC88A* did not reduce GIV transfer (Figure 6E; lane 4). However, MCF7 cells co-cultured with HS5-shGIV cells did not demonstrate GIV protein transfer (Figure 6E; lane 5). Because MCF7 cells expressing shGIV continued to express GIV protein, findings indicate that the observed upregulation of GIV in MCF7 cells in contact culture with HS5 cells relies predominantly on transfer of GIV protein. Some transfer of GIV as mRNA cannot be ruled out.

Cx43 and GIV interact and are co-transported through intercellular communication sites. Because gap junctions serve as sites for

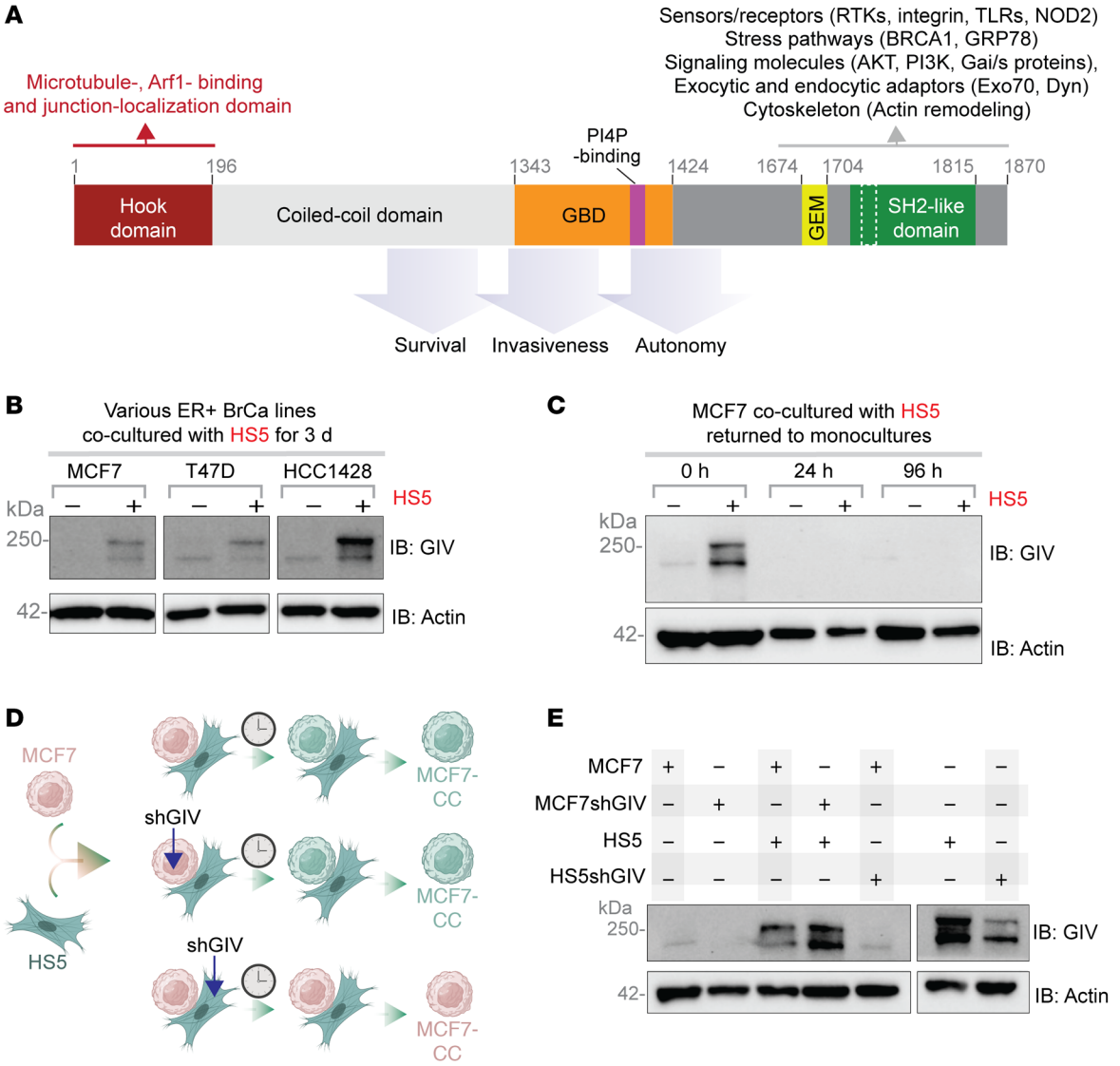

Figure 6. Transfer of GIV from MSCs to ER+ breast cancer cells requires ongoing interactions. (**A**) Schematic illustrates key functional domains of GIV. The C-terminus contains multiple short linear motifs that enable diverse tumor-promoting interactions (receptors, signaling molecules within diverse pathways, and components of membrane trafficking). GBD, G protein–binding domain; GEM, guanine nucleotide exchange modulator; SH2, Src-like homology domain. (**B**) Equal aliquots of lysates of 3 ER+ breast cancer cells (MCF7, T47D, or HCC1428) in monoculture or recovered after co-culture with HS5 cells were analyzed for GIV and actin (as a loading control) by immunoblotting (IB). (**C**) Equal aliquots of lysates of MCF7 cells prepared either immediately after recovery from co-cultures with HS5 cells (0 hours) or after an additional 24 or 96 hours of culture after removal from HS5 contact were analyzed for GIV and actin (as a loading control) by IB. (**D** and **E**) Schematic (**D**) outlines the key manipulations (i.e., treatment with shRNA for GIV) done to either MCF7 or HS5 cells in contact co-cultures. Equal aliquots of MCF7 cells recovered from the co-cultures (left) or HS5 cells in monocultures were analyzed for GIV and actin (loading control) by IB.

TNT formation and/or attachment (30, 54) and CX43 is a shared molecular entity for both, we assessed CX43 expression in MCF7 cells that were either in monocultures or recovered from contact cultures with HS5 cells. Co-culture with HS5 cells increased CX43 in MCF7 cells, while monocultures of MCF7 cells showed undetectable levels of this protein (Figure 7A). Next, we used 2 perturbagens to disrupt intercellular communication via gap junctions: (a) carbenoxolone, a widely used chemical inhibitor of GJIC; and (b) fulvestrant, which inhibits transcription of ER targets, including CX43 (55, 56). Both perturbagens virtually eliminated upregulation of GIV and CX43 in MCF7 cells co-cultured with HS5 cells (Figure 7B), while these compounds had minimal effects on CX43 in HS5 cells alone except at 50 μM carbenoxolone (Supplemental Figure 5). These results show that MCF7 cells require direct, CX43-mediated intercellular communication to borrow GIV protein from HS5 cells.

To resolve the nature of these CX43-dependent compartments that facilitate intercellular communication, we carried out ultrastructural analysis by immunogold electron microscopy. CX43 and GIV co-localized near gap junctions (Figure 7C), at/near more elaborate and less defined contact sites (Figure 7C), or within tube like passages connecting cells (Figure 7C).

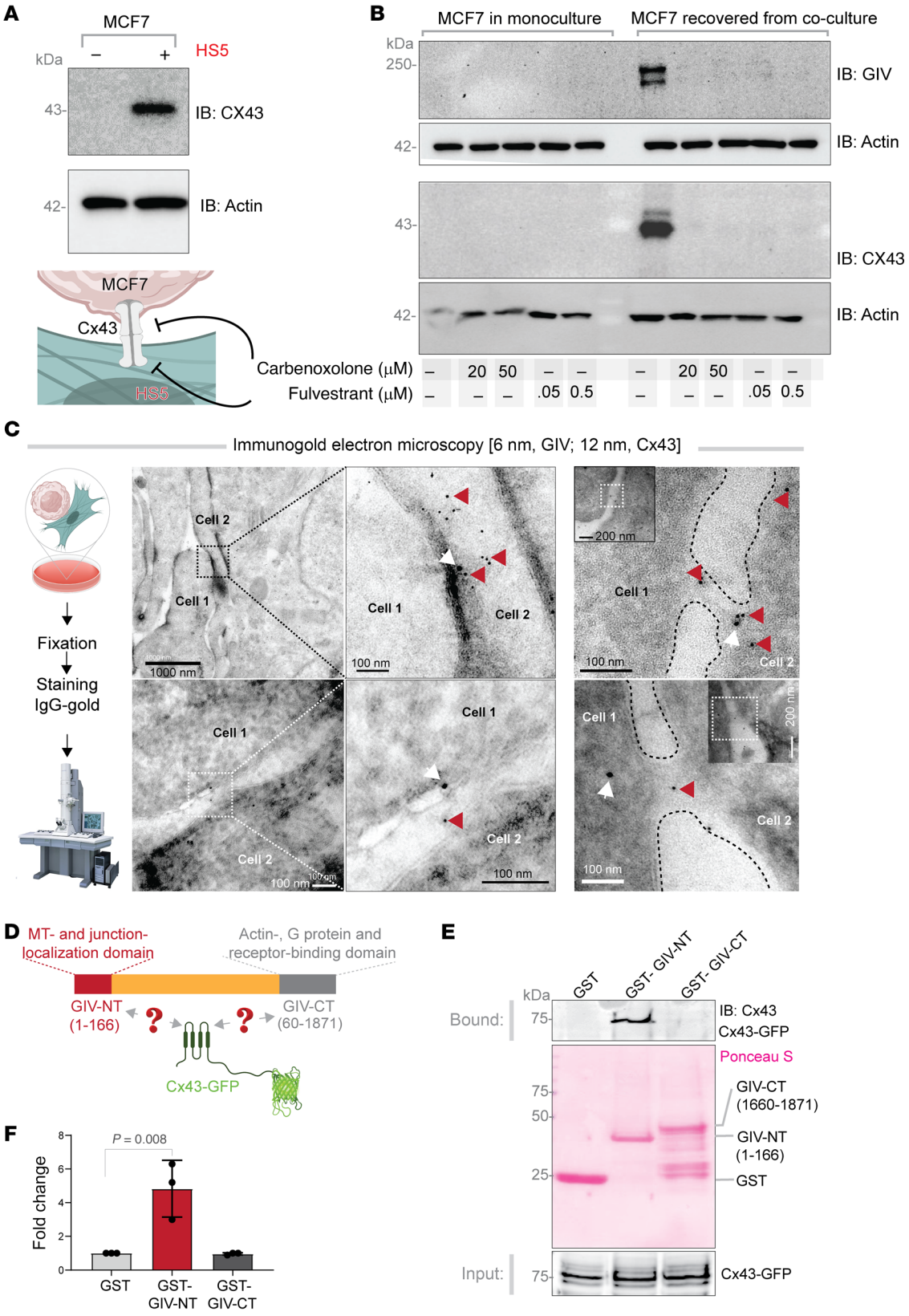
A
MCF7
HS5
kDa
IB: CX43
IB: Actin
MCF7
Cx43
HS5
B
MCF7 in monoculture
MCF7 recovered from co-culture
kDa
IB: GIV
IB: Actin
IB: CX43
IB: Actin
Carbenoxolone (μM)
Fulvestrant (μM)
C
Immunogold electron microscopy [6 nm, GIV; 12 nm, Cx43]
Fixation
Staining
IgG-gold
Cell 1
Cell 2
1000 nm
100 nm
200 nm
D
MT- and junction-localization domain
Actin-, G protein and receptor-binding domain
GIV-NT (1-166)
GIV-CT (60-1871)
Cx43-GFP
E
GST
GST- GIV-NT
GST- GIV-CT
kDa
Bound:
IB: Cx43
Cx43-GFP
Ponceau S
GIV-CT (1660-1871)
GIV-NT (1-166)
GST
Input:
Cx43-GFP
F
P = 0.008
Fold change
GST
GST-GIV-NT
GST-GIV-CT

Figure 7. Cx43 and GIV interact and are co-transported through intercellular communication sites. (**A**) Equal aliquots of lysates of MCF7 cells in monoculture or recovered after co-culture with HS5 cells were analyzed for Cx43 and actin (as a loading control) by immunoblotting (IB). (**B**) MCF7 cells in monoculture or in co-culture with HS5 cells were treated with the indicated concentrations of carbenoxolone or fulvestrant prior to lysis. Equal aliquots of lysates were analyzed for GIV, Cx43 or actin (the latter as a loading control) by IB. See Supplemental Figure 5 for similar studies on HS5 monocultures. (**C**) Electron micrographs of immunogold stained MCF7↔HS5 contact co-cultures. Red arrowhead denotes 6 nm gold particles (GIV); white arrow denotes 12 nm gold particles (Cx43). Scale bar: 1000 nm (top left), 100 nm (bottom left, middle and right panels), 200 nm (right panel insets). (**D**) Schematic of constructs used in pull-down assays with recombinant GST-tagged GIV N- or C-terminal fragments or GST alone (negative control) proteins immobilized on glutathione beads and lysates of Cos7 cells transiently expressing GFP-Cx43. (**E**) Bound Cx43 was visualized by IB (top). Equal loading of GST proteins was confirmed by ponceau S staining (bottom). (**F**) Bar graphs display the relative binding of Cx43 to various GST proteins. Data are represented as mean ± SEM (n = 3); P value determined by 1-way ANOVA with Tukey's HSD test for post hoc pairwise comparisons.

Co-localization of CX43 and GIV suggested that these proteins interact. Using CX43-GFP expressed in Cos7 cells and purified GST fusions of the N-terminal or C-terminal part of GIV in pull-down assays, we confirmed that the N-terminus, but not the C-terminus of GIV binds directly to CX43 (Figure 7, D–F). This finding is consistent with prior work demonstrating the importance of GIV-NT in junctional localization (57).

Together, these findings suggest that CX43 and GIV interact and co-migrate from MSCs to ER+ breast cancer cells during CX43-mediated intercellular transport.

Adding GIV to ER+ breast cancer cells recapitulates key functions gained during contact culture. We asked to what extent GIV alone accounts for or recapitulates functions gained by ER+ breast cancer cells during contact culture with MSCs. We generated MCF7 cells stably expressing GIV and confirmed that exogenous expression produced levels of GIV comparable to that from intercellular transfer from HS5 cells in contact co-cultures (Figure 8A) (Supplemental Figure 6A). RNA sequencing of MCF7-GIV cells revealed that approximately 20% of the genes in the borrowed (n = 32 genes) and intrinsic response (n = 17 genes) components of contact culture perfectly classified MCF7 cells with or without GIV (Figure 8, B and C). We present a complete catalog of these genes in Supplemental Data Set 4. Heatmaps display the differential expression of these genes (Figure 8, E and F). Of the tumor-intrinsic gene response, we previously discovered that co-culture with MSCs upregulated *LCN2*, an iron sequestering protein, and *CD44*, a marker of stem-like cells, in breast cancer cells (19). Pathway analysis of the 32-gene borrowed signature recapitulated by stable expression of GIV alone showed enrichment for numerous processes related to response to external stimuli, while the 17-gene signature included vesicular transport and exocytosis (Supplemental Figure 6, B and C). These data reinforce our focus on GIV within the list of genes transferred from MSCs to breast cancer cells in bone marrow to enhance aggressive traits and facilitate disease progression.

To investigate effects of GIV on drug resistance, we focused on anti-estrogen drugs tamoxifen (a selective estrogen receptor modulator) (58) and fulvestrant (a selective estrogen receptor degrader) (59). We also tested combination therapy with fulvestrant and palbociclib, an inhibitor of CDK4/6 used with anti-estrogen therapy for patients with metastatic ER+ breast cancer. Following 3 days of treatment in low serum, physiologic glucose medium, we quantified relative numbers of viable cells at various concentrations of tamoxifen, fulvestrant, or fulvestrant plus a fixed concentration of palbociclib. MCF7-GIV cells showed resistance to each of these treatment regimens, particularly fulvestrant (Figure 8, G–I). These data establish that GIV confers resistance to clinically used drugs for ER+ breast cancer and suggest that upregulation of GIV in cancer cells in close contact with MSCs may permit disseminated ER+ breast cancer cells to survive therapy in bone marrow.

Because GIV coordinates intracellular signaling pathways enabling growth factor–autonomous survival and proliferation of circulating tumor cells (32, 60), we investigated effects of GIV on hematogenous dissemination of ER+ breast cancer cells. We injected MCF7 and MCF7-GIV cells into the left cardiac ventricle of female immunodeficient NOD.Cg-Prkdc scid (NSG) mice and tracked cancer cells using bioluminescence (Figure 8, J and K). Viable MCF7 cells dropped steadily from day 1 through day 10, while no significant decrease occurred in mice injected with MCF7-GIV cells. From days 0 to 1, signal from control MCF7 cells decreased by approximately 70%, while MCF7-GIV cells diminished by only approximately 10%. From days 1 to 3, losses of viable cells were approximately 20% and less than 10% for MCF7 and MCF7-GIV cells, respectively. The rapid drop in MCF7 cells is not unexpected because we did not supplement mice with estrogen, which typically is required for MCF7 cells to proliferate in vivo. Intriguingly, we noted that differences between groups diminished over time from days 10 to 24 and became virtually indistinguishable thereafter. These results reveal that GIV facilitates survival during the early stages in dissemination of ER+ breast cancer cells. Because contact culture studies in vitro take approximately 3 days to transfer GIV, it is possible that MCF7 cells borrowed GIV from stromal cells that have abundant amounts of the protein.

Tumor cells may acquire CCDC88A and other borrowed genes also from fibroblasts. Studies have documented that disseminated tumor cells and metastases in one organ can seed metastases in a second site, emphasizing the need to understand how the bone marrow environment promotes aggressive phenotypes in breast cancer (61). We asked whether the catalog of borrowed genes we describe here maintained relevance beyond MSCs and extended also to MSCs that can be recruited to the tumors where they give rise to cancer-associated fibroblasts (CAFs (62–64)). CAFs establish TNTs with cancer cells (65), express high levels of GIV, and rely upon GIV to aid cancer progression (66). We leveraged the only publicly available, published study that compared monocultures of MCF7 cells with contact cultures of MCF7 cells and BJ fibroblasts by RNA sequencing (67). As a third comparator group, this prior study cultured MCF7 cells in extracellular matrix (ECM) derived from conditioned media from the BJ fibroblasts (Figure 9A). Contact culture, but not ECM-treated growth conditions, induced each of the 3 borrowed gene signatures we described earlier (Figure 9, B–F). Most importantly, *CCDC88A* was among the borrowed gene signature induced during contact culture with fibroblasts. Furthermore, we found that xenografted tumor cells depleted of GIV by CRISPR/Cas9 (Supplemental Figure 7, A and B) gained GIV protein (Supplemental Figure 7C), but not mRNA

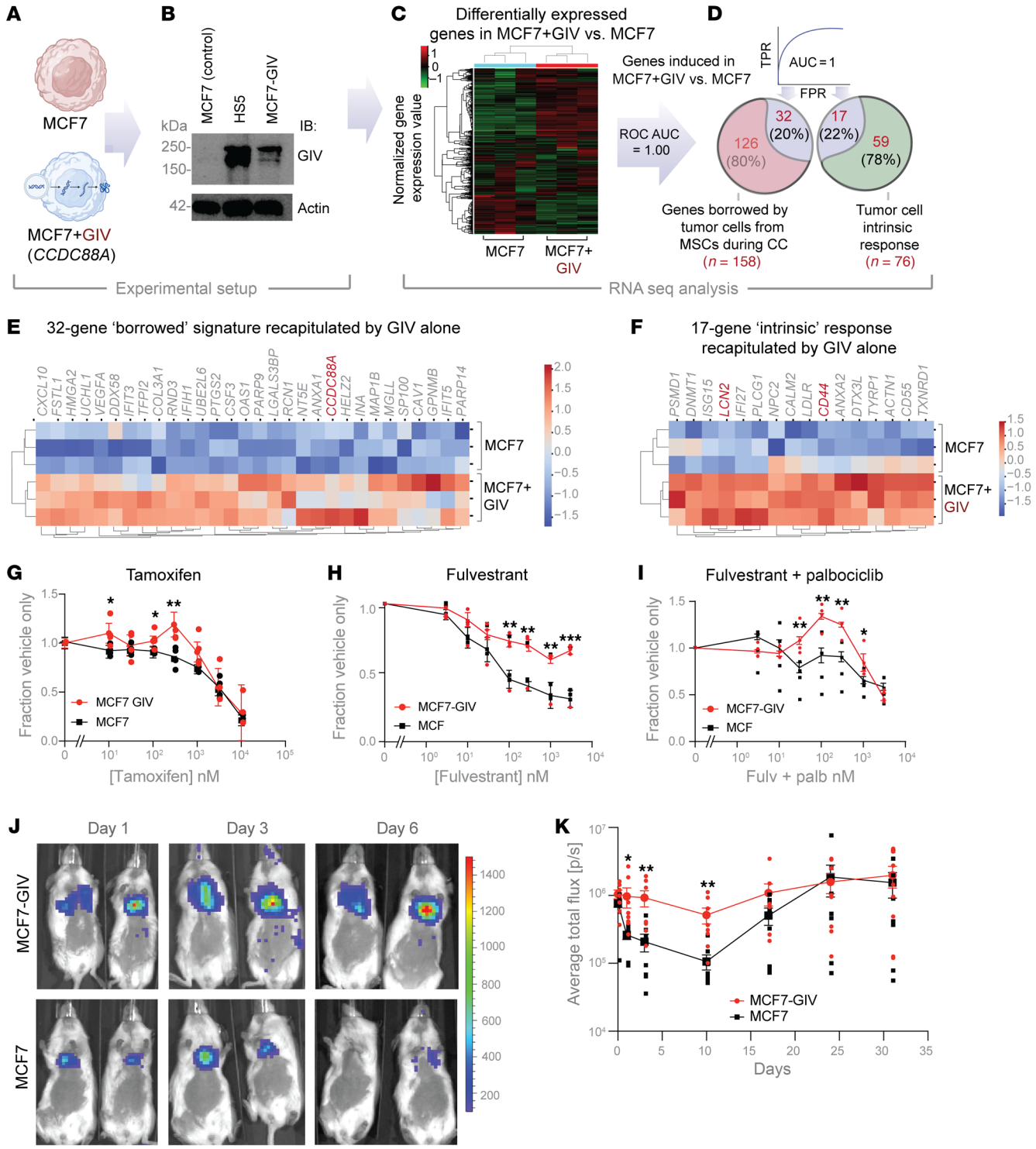

Figure 8. Expression of GIV recapitulates the MSC close contact signature, confers resistance to ER-targeted therapies, and promotes early dissemination of ER+ breast cancer cells. (**A**) Schematic shows creation of a stable MCF7 cell population expressing exogenous GIV (*CCDC88A*) by a piggyBac transposase vector. (**B**) Immunoblots of whole cell lysates of cells in **A**, confirming expression of full-length GIV. (**C** and **D**) Workflow (**C**) of RNA sequencing and normalized gene expression analysis of cells in **B** analyzed for the borrowed (n = 158) and intrinsic (n = 76) genes to perfectly classify MCF7-GIV cells from control MCF7 (ROC-AUC 1.00). Venn diagram (**D**) shows genes induced with GIV alone as percentage of the total borrowed and intrinsic signatures. (**E** and **F**) Heatmaps display hierarchical unsupervised clustering of MCF7 and MCF7-GIV cells by z score–normalized gene expression for the subset of genes induced among the borrowed (**E**) and intrinsic (**F**) signatures. Supplemental Figure 6 shows Reactome pathway analysis of these genes. (**G**–**I**) Graphs display viability for MCF7-GIV and control MCF7 cells exposed to increasing concentrations of tamoxifen (**G**), fulvestrant (**H**), or fulvestrant and 100 nM palpociclib (**I**). Data are displayed after normalization to cells treated with vehicle only. (**J** and **K**) Equal number (1×10^5) of MCF7-GIV or control MCF7 cells were injected into the left cardiac ventricle of 7- to 10-week-old female NSG mice (n = 8 per group). Representative bioluminescence images (**J**) show mice at days 1, 3, and 6 after injection. In **G**–**I** and **K**, graphs show mean values ± SEM of each group at specific data points. Statistical significance between 2 groups at each time point was computed using repeated measures ANOVA. $^*P < 0.1$, $^{**}P \leq 0.05$, $^{***}P \leq 0.01$ indicates corrected P values using Tukey's method.

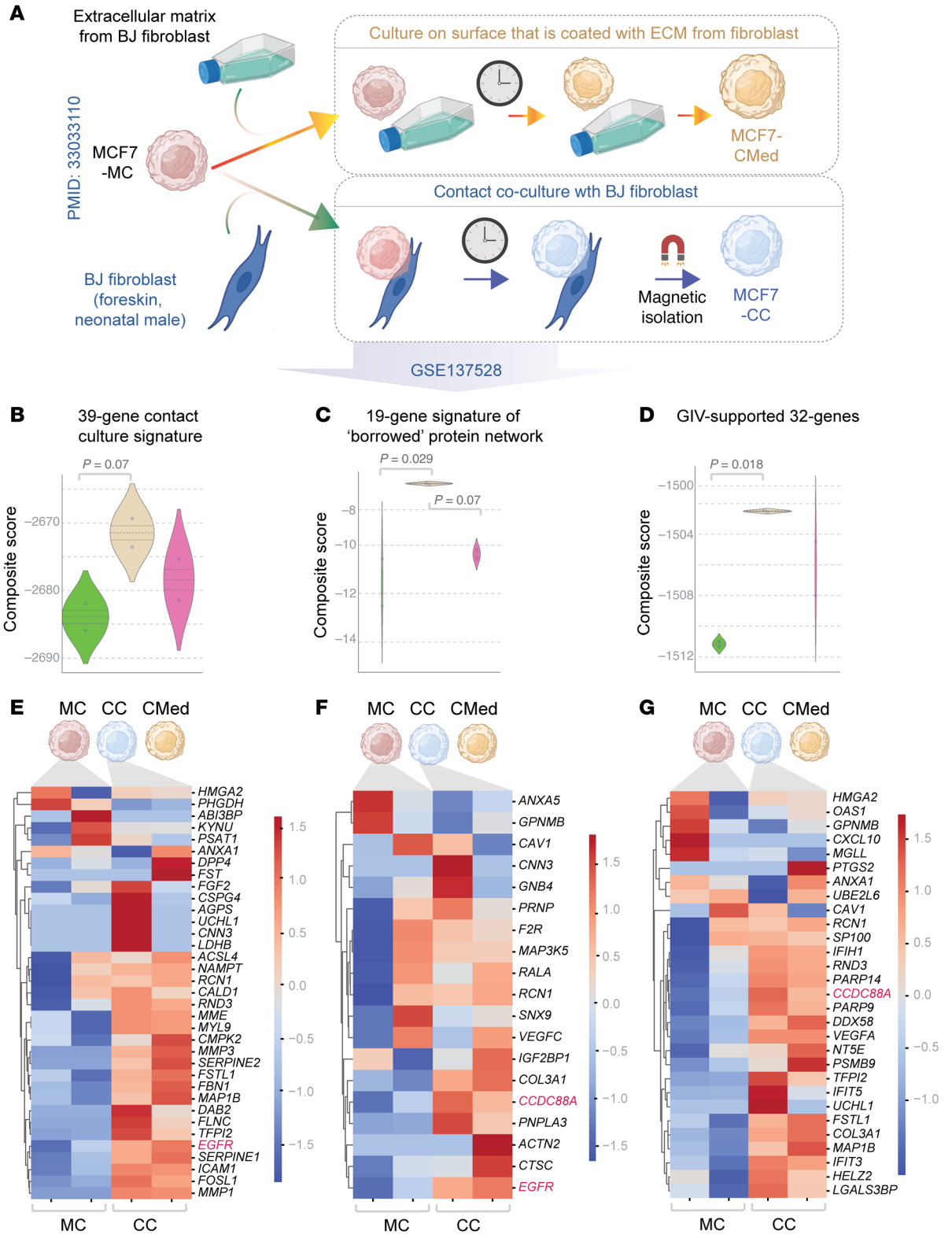

Figure 9. MCF7 cells borrow *CCDC88A* and other key genes during contact culture with fibroblasts. (**A**) Schematic of the experimental setup in which MCF7 cells were grown either as monoculture (MC), or in direct contact cultures with BJ fibroblasts (CC) or cultured on ECM produced by the BJ fibroblasts (CMed). (**B**–**D**) Violin plots show the degrees of induction of 39-gene 2D contact culture signature (**B**), the 19-gene signature of network of borrowed proteins/transcripts that survived refinement through 3D contact cultures (**C**), and GIV-supported borrowed transcriptional program of 32 genes (as in Figure 8D). Statistical significance was assessed by 1-way ANOVA and the *P* values were corrected for multiple comparisons by using Tukey's method. (**E**–**G**) Heatmaps show the induction pattern of each gene within the signatures described in **B**–**D**. Color key denotes *z* score–normalized counts per million (cpm).

(Supplemental Figure 7D), presumably from high-GIV-expressing mouse stromal cells and/or co-implanted human mammary fibroblasts (arrows, Supplemental Figure 7C). These results suggest that ER+ tumor cells may acquire GIV via intercellular transport from diverse stromal cells that express GIV at high levels. This raises the possibility that the phenomenon of GIV acquisition via TNTs may not be limited to bone marrow, but extend also to the primary and metastatic sites, where prolonged contact and transfer could occur between tumor cells and CAFs. It also provides the basis for the observed prognostic significance of the 39-gene signature in ER+ primary tumors (Figure 3, B and F).

Discussion

The major problem we address here is the widely recognized, but poorly understood, means by which bone marrow harbors disseminated tumor cells in ER+ breast cancer, permitting long-term survival of these cells despite hormone targeted therapy (68). Persistence of disseminated tumor cells poses a documented, progressively increasing risk of delayed recurrence that most often occurs in bone (69–71) (~50%) for patients with ER+ breast cancer. MSCs have been implicated as key enablers of tumor cells in the bone marrow niche (61, 72). However, mechanisms that support disseminated tumor cells in bone marrow and potentiate potential recurrence remain unclear. The compendium of TNT tumor-stromal transport we reveal here provides a wealth of potentially actionable targets to disrupt MSC niches for cancer cells and end the current impasse in treating bone metastases. There are potentially three major ways in which this work advances the field of cancer biology.

A catalog of MCS-to-tumor gene transfer. First, we presented an integrated omics workflow that identifies meaningful hits by optimally leveraging the sensitivity (transcriptomics) and specificity (proteomics) of approaches and maintains the relevance and context (2D and 3D datasets). The workflow generated a comprehensive catalog of genes transferred from MSCs to ER+ breast cancer cells during direct contact culture. The approach ensured that low levels of borrowed proteins (such as Cx43 and GIV) were not overlooked due to limitations of proteomics, whereas the 2D versus 3D comparisons ensured that the catalog is likely to be physiologically relevant and reproducible. The multiomic rigor we employed went beyond our own datasets generated using all 4 possible combinations of 2 ER+ breast cancer cell lines and 2 MSC lines. This catalog not only provides a prioritized list of genes for the scientific community to pursue but also provides knowledge of molecular mechanisms that reprogram breast cancer cells in bone marrow. For example, while MSCs regulate breast cancer cells through soluble mediators such as cytokines (73), work done by others and us revealed that key functional changes in ER+ breast cancer cells required direct close contact with MSCs (72). The present catalog provides a multiomic resource to begin to dissect how MSCs shape disease phenotypes in ER+ breast cancer and to what extent effects rely upon intercellular transfer of key molecules (borrowed). We show that the borrowed components integrate seamlessly with a second set of gene expression changes that reflect the cancer cell–intrinsic responses; together, they establish a robust connectome. Key borrowed components belong to the growth factor and prosurvival PI3K/Akt signaling pathways, while the key intrinsic response is augmentation of VEGF signaling, which supports proliferation and angiogenesis. The key process suppressed is dependance on estrogen signaling, consistent with environmentally mediated resistance to hormone targeted therapies (74). The borrowed gene signature showed demonstrable translational relevance in that it prognosticated and predicted outcome in patients with ER+ breast cancers, especially those with treatment-resistant disease. We conclude that the catalog of genes may represent high value targets for preventing MSCs from empowering tumor cells that lie in the bone marrow niche. Contact co-culture of ER+ breast cancer cells and fibroblasts reproducibly upregulated several key genes from this list, implying that findings may have broader relevance in the context of cancer cells in other tissues. Resistance to therapies for ER+ breast cancer and enhanced survival of disseminated MCF7 cells stably expressing GIV recapitulate key features of MCF7 cells in co-culture with MSCs that we reported previously (19, 21), and future studies will delineate whether and how GIV alone may impact additional reported phenotypes, i.e., metabolic plasticity (20).

Gene transfer occurs through a nanotube-based connectivity grid. Second, the catalog of genes provides valuable clues into the predominant mode of intercellular communication between MSCs and tumor cells. Intercellular protein transfer encompasses several different biologic processes and cellular structures that establish dynamic communication networks among cells in direct contact or proximity: Gap junctions, TNTs, extracellular vesicles, trogocytosis, and direct cell fusion are among such processes (75). GO analyses of our catalog of borrowed genes hinted at formation of extracellular tube-like structures, such as TNTs, as a likely mode of transport. This is consistent with prior reports of MSCs establishing TNTs with multiple types of cancer cells, including MCF7 and other breast cancer cell lines (76). Discovered originally in 2004 (14) and critiqued initially by some as artifacts of 2D culture (77), TNTs are now increasingly recognized as conduits for cell-cell communication in both physiology and disease (28, 30, 54, 78). TNTs are F-actin–rich structures with junctional proteins at one end (79, 80); TNTs couple with adjacent cells through gap junctions (81–84), and both share CX43 as common molecular component. We observed formation of abundant TNTs connecting MCF7 cells with MSCs and demonstrated that they are functional using pharmacologic inhibitors, implicating gap junctions and CX43 as facilitators of transport in our cultures. The presence of EGFR on the list of borrowed genes is intriguing. While we did not investigate transfer of this receptor as RNA or protein, transmembrane and membrane bound proteins have previously been reported to be transferred via TNTs (85). Most of the borrowed genes, however, represent cytoplasmic proteins and/or organelle- or cytoskeleton-associated proteins, which are known to use TNTs as a route for intercellular protein transfer (30, 54, 78). That the 483 borrowed genes carried an overwhelming message of intercellular transport structures (tube morphogenesis and development) suggests selection of these genes by their ability to facilitate or support TNT formation, stabilization, and transport. Integration of the borrowed and intrinsic genes through PPI networks indicates that the nature of the exchange is meaningful and advantageous to cancer cells (and potentially also to MSCs). The TNT-dependent tumor-MSC communication we reveal here resembles nanotubes (86, 87) and pili-dependent communication in pathogenic biofilm-producing microbes (which are responsible

for approximately 80% of chronic infectious diseases) (88). Unicellular pathogens deploy these structures to communicate with each other, diverse host cells, or other pathogens to ultimately produce an extracellular grid to adopt a multicellular lifestyle (89, 90). Such adaptation promotes drug resistance, survival, transfer of resistance genes, and metabolic dormancy, in effect, making bacterial biofilms more difficult to eradicate than when present as unicellular organisms (reviewed in refs. 91, 92).

Acquisition of GIV exemplifies how nanotube-dependent gene transfer benefits cancers. Third, our bioinformatic analyses pipeline helped prioritize 1 borrowed gene, *CCDC88A*/GIV, from a list of several interesting candidates. We rationalized GIV because of its known protumorigenic properties (outlined earlier in Results) and because we found it intriguing that the ER+ breast cancer cells typically silence this gene through alternative splicing (51), only to "borrow" it back from MSCs later in the bone marrow niche (this work). We show transfer of GIV primarily as protein (not RNA). Because protein transfer is not driven by gradients and instead relies upon mechanisms of sorting and selective exchange, what governs selectivity of the borrowed proteins remains unclear. For GIV, we show that it binds and co-localizes with CX43 near gap junctions and within TNTs. The 2 proteins co-transfer from MSCs to cancer cells in ways that require functional gap junctions. Discovered originally as an actin binding/remodeling protein in breast cancers (50, 51) and found later to directly bind microtubules and localize to cell junctions under bioenergetic stress (57), both actin and microtubule filaments may serve as highways for transport of GIV between MSCs and cancer cells, as described previously for motor proteins (15) within TNTs. Alternatively, because GIV associates with and regulates functions and/or localization of diverse cellular organelles — ERGIC-Golgi vesicles (93), exocytic vesicles (94), endosomes (94, 95), autophagosomes (96) — and cell surface receptors (e.g., EGFR, integrins, TLR4 etc.) (97), co-transport with such organelles or membrane proteins is also possible. While we did not resolve which of these mechanisms of transfer occur, we assessed the impact of GIV transfer.

By stably expressing GIV alone (among the list of borrowed candidates) in an ER+ breast cancer cell line, we recapitulated approximately 20% of the gene expression patterns within the borrowed and intrinsic response components. Expression of GIV in ER+ breast cancer cells conferred resistance to clinical antiestrogen drugs and promoted early survival and dissemination of circulating breast cancer cells. *CCDC88A*/GIV is also induced in ER+ breast cancer cells in contact cultures with fibroblasts, keeping with prior work demonstrating the role of GIV in cancer-associated fibroblasts in the dissemination of cancer (66). MSCs and other sources of carcinoma-associated fibroblasts in primary breast tumors potentially may donate GIV to ER+ breast cancer cells, priming cancer cells to survive in the circulation and disseminate to bone marrow. Given the short-lived duration of GIV in recipient breast cancer cells after separation from MSCs we observed in our studies (Figure 6E), ER+ breast cancer cells upon landing in the bone marrow may then need to re-establish contacts with MSCs in bone marrow to maintain expression of GIV. Considering recent revelations that GIV scaffolds a circuit for secretion coupled cellular autonomy (or growth signaling autonomy) in multicellular eukaryotic cells (32), it is possible that sharing of GIV between haves (stromal cells) and have-nots (tumors that are originally GIV-negative) as ready-to-use protein reflects a core biological phenomenon of sharing of resources during an urgent need for survival in growth factor restrictive environments. Transfer as protein bypasses the need for energy expenditure for protein translation and yet achieves higher levels of protein than possible through mRNA transfer; the latter is estimated to be never more than 1% of levels in donor cells (98). Although we found that GIV protein acquired during 3 days in contact culture was rapidly lost after returning cancer cells to monoculture, prolonged contact cultures (for months and years, as happens in patients) may allow transferred GIV to initiate the GIV↔STAT3 feedforward loop shown to enhance its own transcription (99) and, thereby, sustain its levels in cells. If so, GIV may promote further "social" interactions and "exchanges" with bone marrow MSCs through augmentation of TNT formation to facilitate its spread across tumor masses as tumors grow. This is not entirely unexpected given the distinct microtubule and actin-binding modules present in GIV and its known functions in vesicle transport, all aspects that are critical for active transport via TNTs (30, 54). We also noted that GIV mRNA was elevated in contact cultures, suggesting that acquisition of some GIV as mRNA or its induction as an intrinsic tumor cell response to the borrowed proteins likely occurs. We conclude that intercellular protein transport is a major way for cells to exchange GIV as an essential commodity within a heterotypic population of haves and have-nots.

Study limitations. A limitation of this study is the use of a conditioned medium from MSCs rather than contact-free co-cultures with separation of cell types in Transwells. Although such a setup may have enabled assessment of bidirectional crosstalk in which ER+ tumor cells could initiate or perpetuate the effects of MSCs on cancer cells, Transwell setups present substantial technical challenges and risk a major confounding factor. For example, it is challenging to collect sufficient cells for RNA sequencing and proteomics from Transwells, and prolonged (72 hours) cultures risk the formation of gradients of secreted growth factors and/or chemokines that could trigger migration across the insert and direct contact between cell types. Also, we did not pursue detailed characterization of all that is transported. Some genes are likely to be transported from cancer cells to MSCs; we did not evaluate this here. Contact culture induced tolerant immunogenic signals in cancer cells; how these signals impact immune evasion by cancer cells and/or resistance to immune checkpoint blockade therapies will require further studies in immunocompetent mice. TNT-mediated tumor-CAF exchanges also shape tumor cell behaviors (65, 100); dedicated studies are required to further investigate the shared and distinct patterns between these (and potentially others, e.g., tumor-myeloid cell) forms of cell-cell communication. Further studies also are needed to establish mechanisms initiating and sustaining TNT communication between cancer and stromal cells and whether the nature and extent of the TNT-facilitated exchange described here also occur in more complex systems, such as patient-derived organoids cultured in 3D under near-physiologic conditions in the presence of immune and non-immune cells. Furthermore, we did not distinguish which RNAs and proteins presumed to be borrowed from MSCs by ER+ breast cancer cells are directly transferred as opposed to reflecting secondary changes induced by a subset of the borrowed molecules. Regard-

less of the relative contributions of these subsets, the induced transcriptome-proteome carries meaningful information regarding tumor growth, resistance, and relapse.

In conclusion, this work provides insights into how close contact interactions and intercellular communication networks through RNA/protein transfer between ER+ breast cancer cells and MSCs reprogram tumor cells to more aggressive states. Based on the omics-based revelations and experimental evidence (this work) and phenotypic characterization of MSC-tumor contact culture we published earlier (68), we conclude that TNT-based cell-cell communication in the bone marrow niche (or tumor-stromal or tumor-immune cell communication in any other tissue) may provide the same to cancer cells that nanotube-based communication provides to the bacteria within biofilms; a nutrition- and metabolic stress-free haven to promote sustained survival in new environments. Blocking or redirecting these communication networks, or components transferred through these networks, offers promising opportunities to prevent or cure breast cancer metastasis to bone.

Methods

Sex as a biologic variable. All animal experiments used only female mice because 99% of breast cancers occur in women.

RNA sequencing and DEG analysis. Genes with a log(fold change) of 2 or greater and adjusted *P* value of less than 0.05 were identified and rank ordered as DEGs (Supplemental Data Set 5). Besides the datasets generated in this work, we leveraged several publicly available datasets. A complete inventory of these datasets and their nature, composition, and source is presented in Supplemental Data Set 7.

Tandem mass tag proteomics and analyses. We deposited mass spectrometry proteomics data in the ProteomeXchange Consortium via the PRIDE (101) partner repository with the dataset identifier (PXD039860). A list of differentially expressed proteins is provided in Supplemental Data Set 6.

Study approval. The University of Michigan IACUC approved all animal procedures under protocol number PRO00010534.

Data availability. Data are available via ProteomXchange with identifier PDX039860 and the NCBI Gene Expression Omnibus with the identifier GSE224322. The computational analyses can be found at https://github.com/sinha7290/cx43. Values for all data points in graphs are reported in the Supporting Data Values file. Supplemental Methods contains further information about experimental and computational procedures.

Author contributions

SS, supervised by PG, carried out and analyzed all electron microscopy, RNA seq, TMT proteomics and computational analyses showcased in this work. S Roy carried out protein purification and GST pulldown assays. BWC, APF, SC, S Rajendran, and JMB performed mouse experiments and cell-based assays. KEL provided reagents. MM provided expertise in statistical analysis. BWC, SS, PG, and GDL assembled the figures. KEL, S Roy, SS, PG, and GDL helped write methods and edit the manuscript. GDL and PG conceptualized, designed, supervised, and analyzed the experiments. KEL, SS, PG, and GDL wrote the manuscript. All authors approved the manuscript prior to submission.

Acknowledgments

The authors acknowledge funding from United States National Institute of Health grants R01CA238042 (to PG and GDL); R01CA100768, R01CA160911 (to PG); R50CA221807 (to KEL) and U01CA210152, R01CA238023, R33CA225549, and R37CA222563 (to GDL). We also acknowledge support from the Padres Pedal the Cause PTC2021 and the Torey Coast Foundation, La Jolla (to PG) and the W.M. Keck Foundation (to GDL). SS was supported in part by the American Association of Immunologists' (AAI) Intersect Fellowship Program for Computational Scientists and Immunologists. We thank Guillaume Castillon (UC San Diego Electron Microscopy Core Facility) for technical and logistical support. This manuscript includes data generated at the UC San Diego Institute of Genomic Medicine (IGM) using an Illumina NovaSeq 6000 that was purchased with funding from an NIH SIG grant (S10 OD026929). The manuscript also includes data generated through the University of Michigan Advanced Genomics, Flow Cytometry, and Pre-Clinical Imaging shared resources supported in part by the University of Michigan Comprehensive Cancer Center support grant P30CA046592.

Address correspondence to: Pradipta Ghosh, Departments of Medicine and Cellular and Molecular Medicine, University of California San Diego, 9500 Gilman Drive (MC 0651), George E. Palade Bldg, Rm 232, 239, La Jolla, California 92093, USA. Phone: 858.822.7633; Email: prghosh@ucsd.edu. Or to: Gary D. Luker, Departments of Radiology and Biomedical Engineering, A524 BSRB, 109 Zina Pitcher Place, Ann Arbor, Michigan 48109-2200, USA. Phone: 734.764.2890; Email: gluker@umich.edu.

1. Kennecke H, et al. Metastatic behavior of breast cancer subtypes. *J Clin Oncol*. 2010;28(20):3271–3277.
2. Coleman RE, et al. Bone metastases. *Nat Rev Dis Primers*. 2020;6(1):83.
3. Weilbaecher KN, et al. Cancer to bone: a fatal attraction. *Nat Rev Cancer*. 2011;11(6):411–425.
4. Pan H, et al. 20-year risks of breast-cancer recurrence after stopping endocrine therapy at 5 years. *N Engl J Med*. 2017;377(19):1836–1846.
5. Beuzeboc P, Scholl S. Prevention of bone metastases in breast cancer patients. Therapeutic perspectives. *J Clin Med*. 2014;3(2):521–536.
6. Smart E, et al. Update on the role of NFκB in promoting aggressive phenotypes of estrogen receptor-positive breast cancer. *Endocrinology*. 2020;161(10):bqaa152.
7. Abd El-Hafeez AA, et al. Regulation of DNA damage response by trimeric G-proteins. *iScience*. 2023;26(2):105973.
8. Pasquier J, et al. Preferential transfer of mitochondria from endothelial to cancer cells through tunneling nanotubes modulates chemoresistance. *J Transl Med*. 2013;11:94.
9. Imai Y, et al. Angiotensin-converting enzyme 2 protects from severe acute lung failure. *Nature*. 2005;436(7047):112–116.
10. Martin FT, et al. Potential role of mesenchymal stem cells (MSCs) in the breast tumour microenvironment: stimulation of epithelial to mesenchymal transition (EMT). *Breast Cancer Res Treat*. 2010;124(2):317–326.
11. Wang R, et al. Breast cancer MCF-7 cells acquire heterogeneity during successive co-culture with hematopoietic and bone marrow-derived mesenchymal stem/stromal cells. *Cells*. 2022;11(22):3553.
12. Nielsen MS, et al. Gap junctions. *Compr Physiol*. 2012;2(3):1981–2035.
13. Wu JI, Wang LH. Emerging roles of gap junction proteins connexins in cancer metastasis, chemoresistance and clinical application. *J Biomed Sci*. 2019;26(1):8.
14. Rustom A, et al. Nanotubular highways for intercellular organelle transport. *Science*. 2004;303(5660):1007–1010.
15. Gerdes HH, Carvalho RN. Intercellular transfer mediated by tunneling nanotubes. *Curr Opin Cell*

Biol. 2008;20(4):470–475.
16. Lou E, et al. Tunneling nanotubes provide a unique conduit for intercellular transfer of cellular contents in human malignant pleural mesothelioma. *PLoS One*. 2012;7(3):e33093.
17. Hanna SJ, et al. Tunneling nanotubes, a novel mode of tumor cell-macrophage communication in tumor cell invasion. *J Cell Sci*. 2019;132(3):jcs223321.
18. Shiozawa Y, et al. Hematopoietic stem cell niche is a potential therapeutic target for bone metastatic tumors. *Clin Cancer Res*. 2011;17(17):5553–5558.
19. Buschhaus JM, et al. Effects of iron modulation on mesenchymal stem cell-induced drug resistance in estrogen receptor-positive breast cancer. *Oncogene*. 2022;41(29):3705–3718.
20. Buschhaus JM, et al. Bone marrow mesenchymal stem cells induce metabolic plasticity in estrogen receptor-positive breast cancer. *Mol Cancer Res*. 2023;21(5):458–471.
21. Augimeri G, et al. A hybrid breast cancer/mesenchymal stem cell population enhances chemoresistance and metastasis. *JCI Insight*. 2023;8(18):e164216.
22. Kim RS, et al. Dormancy signatures and metastasis in estrogen receptor positive and negative breast cancer. *PLoS One*. 2012;7(4):e35569.
23. Hatzis C, et al. A genomic predictor of response and survival following taxane-anthracycline chemotherapy for invasive breast cancer. *JAMA*. 2011;305(18):1873–1881.
24. Curtis C, et al. The genomic and transcriptomic architecture of 2,000 breast tumours reveals novel subgroups. *Nature*. 2012;486(7403):346–352.
25. Rozanova S, et al. Quantitative mass spectrometry-based proteomics: an overview. *Methods Mol Biol*. 2021;2228:85–116.
26. Pappireddi N, et al. A review on quantitative multiplexed proteomics. *Chembiochem*. 2019;20(10):1210–1224.
27. Laskay UA, et al. Practical considerations for improving the productivity of mass spectrometry-based proteomics. *Chimia (Aarau)*. 2013;67(4):244–249.
28. Tishchenko A, et al. Cx43 and associated cell signaling pathways regulate tunneling nanotubes in breast cancer cells. *Cancers (Basel)*. 2020;12(10):2798.
29. Dhimolea E, et al. Pleiotropic mechanisms drive endocrine resistance in the three-dimensional bone microenvironment. *Cancer Res*. 2021;81(2):371–383.
30. Cordero Cervantes D, Zurzolo C. Peering into tunneling nanotubes-The path forward. *EMBO J*. 2021;40(8):e105789.
31. Lou E, et al. Lost in translation: applying 2D intercellular communication via tunneling nanotubes in cell culture to physiologically relevant 3D microenvironments. *FEBS J*. 2017;284(5):699–707.
32. Qiao L, et al. A circuit for secretion-coupled cellular autonomy in multicellular eukaryotic cells. *Mol Syst Biol*. 2023;19(4):e11127.
33. Sinha S, et al. Growth signaling autonomy in circulating tumor cells aids metastatic seeding. *PNAS Nexus*. 2024;3(2):pgae014.
34. Datta A, et al. Cytoskeletal dynamics in epithelial-mesenchymal transition: insights into therapeutic targets for cancer metastasis. *Cancers (Basel)*. 2021;13(8):1882.
35. Pastushenko I, et al. Identification of the tumour transition states occurring during EMT. *Nature*. 2018;556(7702):463–468.
36. Gonzalez DM, Medici D. Signaling mechanisms of the epithelial-mesenchymal transition. *Sci Signal*. 2014;7(344):re8.
37. Pastushenko I, Blanpain C. EMT transition states during tumor progression and metastasis. *Trends Cell Biol*. 2019;29(3):212–226.
38. Das V, et al. The basics of epithelial-mesenchymal transition (EMT): A study from a structure, dynamics, and functional perspective. *J Cell Physiol*. 2019;234(9):14535–14555.
39. Pinto G, et al. Tunneling nanotubes: the fuel of tumor progression? *Trends Cancer*. 2020;6(10):874–888.
40. Hase K, et al. M-Sec promotes membrane nanotube formation by interacting with Ral and the exocyst complex. *Nat Cell Biol*. 2009;11(12):1427–1432.
41. Wittig D, et al. Multi-level communication of human retinal pigment epithelial cells via tunneling nanotubes. *PLoS One*. 2012;7(3):e33195.
42. Warawdekar UM. An assay to assess gap junction communication in cell lines. *J Biomol Tech*. 2019;30(1):1–6.
43. Natsume A, et al. Girdin maintains the stemness of glioblastoma stem cells. *Oncogene*. 2012;31(22):2715–2724.
44. Rohena C, et al. GIV•kindlin interaction is required for kindlin-mediated integrin recognition and activation. *iScience*. 2020;23(6):101209.
45. Cao F, et al. Girdin promotes tumorigenesis and chemoresistance in lung adenocarcinoma by interacting with PKM2. *Cancers (Basel)*. 2022;14(22):5688.
46. Midde K, et al. Single-cell imaging of metastatic potential of cancer cells. *iScience*. 2018;10:53–65.
47. Dunkel Y, et al. Prognostic impact of total and tyrosine phosphorylated GIV/Girdin in breast cancers. *FASEB J*. 2016;30(11):3702–3713.
48. Ghosh P. Heterotrimeric G proteins as emerging targets for network based therapy in cancer: End of a long futile campaign striking heads of a Hydra. *Aging (Albany NY)*. 2015;7(7):469–474.
49. Kitamura T, et al. Regulation of VEGF-mediated angiogenesis by the Akt/PKB substrate Girdin. *Nat Cell Biol*. 2008;10(3):329–337.
50. Jiang P, et al. An actin-binding protein Girdin regulates the motility of breast cancer cells. *Cancer Res*. 2008;68(5):1310–1318.
51. Ghosh P, et al. A G{alpha}i-GIV molecular complex binds epidermal growth factor receptor and determines whether cells migrate or proliferate. *Mol Biol Cell*. 2010;21(13):2338–2354.
52. Nishimae K, et al. The impact of Girdin expression on recurrence-free survival in patients with luminal-type breast cancer. *Breast Cancer*. 2015;22(5):445–451.
53. Peng WT, et al. Elevated expression of Girdin in the nucleus indicates worse prognosis for patients with estrogen receptor-positive breast cancer. *Ann Surg Oncol*. 2014;21(suppl 4):S648–S656.
54. Zurzolo C. Tunneling nanotubes: Reshaping connectivity. *Curr Opin Cell Biol*. 2021;71:139–147.
55. Tsai CF, et al. Inhibition of estrogen receptor reduces connexin 43 expression in breast cancers. *Toxicol Appl Pharmacol*. 2018;338:182–190.
56. Ren J, et al. 17β estradiol regulation of connexin 43-based gap junction and mechanosensitivity through classical estrogen receptor pathway in osteocyte-like MLO-Y4 cells. *Bone*. 2013;53(2):587–596.
57. Aznar N, et al. AMP-activated protein kinase fortifies epithelial tight junctions during energetic stress via its effector GIV/Girdin. *Elife*. 2016;5:e20795.
58. Osborne CK. Tamoxifen in the treatment of breast cancer. *N Engl J Med*. 1998;339(22):1609–1618.
59. Osborne CK, et al. Fulvestrant: an oestrogen receptor antagonist with a novel mechanism of action. *Br J Cancer*. 2004;90(suppl 1):S2–S6.
60. Sinha S, et al. Growth signaling autonomy in circulating tumor cells aids metastatic seeding. *PNAS Nexus*. 2024;3(2):pgae014.
61. Yagi H, Kitagawa Y. The role of mesenchymal stem cells in cancer development. *Front Genet*. 2013;4:261.
62. Barcellos-de-Souza P, et al. Mesenchymal stem cells are recruited and activated into carcinoma-associated fibroblasts by prostate cancer microenvironment-derived TGF-β1. *Stem Cells*. 2016;34(10):2536–2547.
63. Weber CE, et al. Osteopontin mediates an MZF1-TGF-β1-dependent transformation of mesenchymal stem cells into cancer-associated fibroblasts in breast cancer. *Oncogene*. 2015;34(37):4821–4833.
64. Yang D, et al. Cancer-associated fibroblasts: from basic science to anticancer therapy. *Exp Mol Med*. 2023;55(7):1322–1332.
65. Ippolito L, et al. Cancer-associated fibroblasts promote prostate cancer malignancy via metabolic rewiring and mitochondrial transfer. *Oncogene*. 2019;38(27):5339–5355.
66. Yamamura Y, et al. Akt-Girdin signaling in cancer-associated fibroblasts contributes to tumor progression. *Cancer Res*. 2015;75(5):813–823.
67. DiGiacomo JW, et al. Extracellular matrix-bound FGF2 mediates estrogen receptor signaling and therapeutic response in breast cancer. *Mol Cancer Res*. 2021;19(1):136–149.
68. Buschhaus JM, et al. Targeting disseminated estrogen-receptor-positive breast cancer cells in bone marrow. *Oncogene*. 2020;39(34):5649–5662.
69. Davies C, et al. Long-term effects of continuing adjuvant tamoxifen to 10 years versus stopping at 5 years after diagnosis of oestrogen receptor-positive breast cancer: ATLAS, a randomised trial. *Lancet*. 2013;381(9869):805–816.
70. Lee SJ, et al. Implications of bone-only metastases in breast cancer: favorable preference with excellent outcomes of hormone receptor positive breast cancer. *Cancer Res Treat*. 2011;43(2):89–95.
71. Zhang XH, et al. Metastasis dormancy in estrogen receptor-positive breast cancer. *Clin Cancer Res*. 2013;19(23):6389–6397.
72. Xuan X, et al. Mesenchymal stem cells in cancer progression and anticancer therapeutic resistance. *Cancer Cell Int*. 2021;21(1):595.
73. Liang W, et al. Mesenchymal stem cells as a double-edged sword in tumor growth: focusing on MSC-derived cytokines. *Cell Mol Biol Lett*. 2021;26(1):3.

74. Shee K, et al. Therapeutically targeting tumor microenvironment-mediated drug resistance in estrogen receptor-positive breast cancer. *J Exp Med*. 2018;215(3):895–910.
75. Ahmed KA, Xiang J. Mechanisms of cellular communication through intercellular protein transfer. *J Cell Mol Med*. 2011;15(7):1458–1473.
76. Vignais ML, et al. Cell connections by tunneling nanotubes: effects of mitochondrial trafficking on target cell metabolism, homeostasis, and response to therapy. *Stem Cells Int*. 2017;2017:6917941.
77. Dubois F, et al. Investigating tunneling nanotubes in cancer cells: guidelines for structural and functional studies through cell imaging. *Biomed Res Int*. 2020;2020:2701345.
78. Han X, Wang X. Opportunities and challenges in tunneling nanotubes research: how far from clinical application? *Int J Mol Sci*. 2021;22(5):2306.
79. Sartori-Rupp A, et al. Correlative cryo-electron microscopy reveals the structure of TNTs in neuronal cells. *Nat Commun*. 2019;10(1):342.
80. Alarcon-Martinez L, et al. Interpericyte tunnelling nanotubes regulate neurovascular coupling. *Nature*. 2020;585(7823):91–95.
81. Wang X, et al. Animal cells connected by nanotubes can be electrically coupled through interposed gap-junction channels. *Proc Natl Acad Sci U S A*. 2010;107(40):17194–17199.
82. Wang X, et al. Developing neurons form transient nanotubes facilitating electrical coupling and calcium signaling with distant astrocytes. *PLoS One*. 2012;7(10):e47429.
83. Lock JT, et al. Communication of Ca(2+) signals via tunneling membrane nanotubes is mediated by transmission of inositol trisphosphate through gap junctions. *Cell Calcium*. 2016;60(4):266–272.
84. Okafo G, et al. Tunneling nanotubes (TNT) mediate long-range gap junctional communication: Implications for HIV cell to cell spread. *Sci Rep*. 2017;7(1):16660.
85. Turos-Korgul L, et al. Tunneling nanotubes facilitate intercellular protein transfer and cell networks function. *Front Cell Dev Biol*. 2022;10:915117.
86. Dubey GP, Ben-Yehuda S. Intercellular nanotubes mediate bacterial communication. *Cell*. 2011;144(4):590–600.
87. Pande S, et al. Metabolic cross-feeding via intercellular nanotubes among bacteria. *Nat Commun*. 2015;6:6238.
88. Koo H, et al. Targeting microbial biofilms: current and prospective therapeutic strategies. *Nat Rev Microbiol*. 2017;15(12):740–755.
89. Claessen D, et al. Bacterial solutions to multicellularity: a tale of biofilms, filaments and fruiting bodies. *Nat Rev Microbiol*. 2014;12(2):115–124.
90. Mandlik A, et al. Pili in Gram-positive bacteria: assembly, involvement in colonization and biofilm development. *Trends Microbiol*. 2008;16(1):33–40.
91. Preda VG, Săndulescu O. Communication is the key: biofilms, quorum sensing, formation and prevention. *Discoveries (Craiova)*. 2019;7(3):e100.
92. Javid B, Derbyshire KM. Nanotubes: shaking hands, talking, or sharing? *Front Microbiol*. 2011;2:95.
93. Lo IC, et al. Activation of Gαi at the Golgi by GIV/Girdin imposes finiteness in Arf1 signaling. *Dev Cell*. 2015;33(2):189–203.
94. Beas AO, et al. Gαs promotes EEA1 endosome maturation and shuts down proliferative signaling through interaction with GIV (Girdin). *Mol Biol Cell*. 2012;23(23):4623–4634.
95. Gupta V, et al. GIV/Girdin activates Gαi and inhibits Gαs via the same motif. *Proc Natl Acad Sci U S A*. 2016;113(39):E5721–E5730.
96. Garcia-Marcos M, et al. A GDI (AGS3) and a GEF (GIV) regulate autophagy by balancing G protein activity and growth factor signals. *Mol Biol Cell*. 2011;22(5):673–686.
97. Ghosh P, Mullick M. Building unconventional G protein-coupled receptors, one block at a time. *Trends Pharmacol Sci*. 2021;42(7):514–517.
98. Dasgupta S, et al. Global analysis of contact-dependent human-to-mouse intercellular mRNA and lncRNA transfer in cell culture. *Elife*. 2023;12:e83584.
99. Dunkel Y, et al. STAT3 protein up-regulates Gα-interacting vesicle-associated protein (GIV)/Girdin expression, and GIV enhances STAT3 activation in a positive feedback loop during wound healing and tumor invasion/metastasis. *J Biol Chem*. 2012;287(50):41667–41683.
100. Fiori ME, et al. Cancer-associated fibroblasts as abettors of tumor progression at the crossroads of EMT and therapy resistance. *Mol Cancer*. 2019;18(1):70.
101. Perez-Riverol Y, et al. The PRIDE database resources in 2022: a hub for mass spectrometry-based proteomics evidences. *Nucleic Acids Res*. 2022;50(d1):D543–D552.